THE JOURNAL OF BIOLOGICAL CHEMISTRY
Vol. 278, No. 38, Issue of September 19, pp. 36430–36434, 2003
Printed in U.S.A.

Crystal Structure of the Amino-terminal Microtubule-binding Domain of End-binding Protein 1 (EB1)*

Received for publication, June 2, 2003, and in revised form, June 17, 2003
Published, JBC Papers in Press, July 11, 2003, DOI 10.1074/jbc.M305773200

Ikuko Hayashi‡ and Mitsuhiko Ikura

From the Division of Molecular and Structural Biology, Ontario Cancer Institute and Department of Medical Biophysics, University of Toronto, Toronto, Ontario M5G 2M9, Canada

The end-binding protein 1 (EB1) family is a highly conserved group of proteins that localizes to the plus-ends of microtubules. EB1 has been shown to play an important role in regulating microtubule dynamics and chromosome segregation, but its regulation mechanism is poorly understood. We have determined the 1.45-Å resolution crystal structure of the amino-terminal domain of EB1, which is essential for microtubule binding, and show that it forms a calponin homology (CH) domain fold that is found in many proteins involved in the actin cytoskeleton. The functional CH domain for actin binding is a tandem pair, whereas EB1 is the first example of a single CH domain that can associate with the microtubule filament. Although our biochemical study shows that microtubule binding of EB1 is electrostatic in part, our mutational analysis suggests that the hydrophobic network, which is partially exposed in our crystal structure, is also important for the association. We propose that, like other actin-binding CH domains, EB1 employs the hydrophobic interaction to bind to microtubules.

Microtubules (MTs)[1] are an essential component of the cytoskeleton, underlying the fundamental processes of cell morphogenesis, cell motility, and cell division. The organization and dynamics of MT polymers are highly regulated, and numerous proteins including MT-associated proteins (MAPs) and molecular motors have been proposed as possible regulatory factors (1).

MTs have an intrinsic structural polarity, consisting of a highly dynamic plus-end toward the cell periphery and a centrosome-associated minus-end. Their dynamics involve alternating phases of growth and shortening, known as dynamic instability (2). Dynamic instability is modulated by various MAPs and motor proteins, some of which act to promote MT assembly and stability, whereas others induce their depolymerization (3). Two groups of proteins that specifically bind to the MT plus-ends, termed "plus-end-tracking proteins" or +TIPs (4) have been identified: the CAP-Gly proteins (*e.g.* CLIP-170, p150^{glued} of dynactin) and the EB1 family proteins (5–7). Although they can bind to MTs independently, evidence for interactions among them have led to the hypothesis of a "plus-end complex" (8, 9). The main function of a plus-end complex may be the regulation of MT dynamics, but the mechanisms are poorly understood.

EB1 was initially identified in a yeast two-hybrid screen by its binding to the carboxyl terminus of the adenomatous polyposis coli (APC) tumor suppressor protein (10), which may be essential for the tumor-suppressing function of APC (11). Proteins homologous to EB1 have been identified in many organisms from yeast to human and have been shown to interact with MT plus-ends (6, 12–15). EB1 binding to MTs is independent of APC, but APC targeting to MT plus-ends requires EB1 (16, 17). In addition, the APC carboxyl terminus cooperates with EB1 functionally to stabilize MTs (18).

Recent biological studies have revealed that EB1 consists of an amino-terminal MT-binding (En) domain and a carboxyl-terminal APC-binding domain (19, 20). To understand the structural basis of EB1 function in MT binding, we have determined the crystal structure of human En (residues Met-1—Arg-130). The unexpected structural similarity with the calponin homology domain led us to test the MT binding of En with mutagenesis, showing that the interaction is both hydrophobic and electrostatic in nature.

EXPERIMENTAL PROCEDURES

Protein Expression and Purification—The human EB1 amino-terminal MT-binding domain (residues 1–130) was generated by PCR from a human adult brain cDNA library and cloned into pET15b vector (Novagen) using *Nde*I and *Xho*I restriction enzyme sites. The recombinant protein with His_6 tag was expressed in *Escherichia coli* strain BL21(DE3). Cell lysate was applied to a nickel-chelating column (Amersham Biosciences). The eluted protein was digested with thrombin protease (Sigma) to remove the His_6 tag and purified by gel filtration (Superdex 75, Amersham Biosciences) with a buffer containing 10 mM Tris, pH 8.0, 0.1 M NaCl and 1 mM dithiothreitol. The protein fractions were pooled, concentrated to 15 mg/ml in the same buffer as in gel filtration, and used for crystallization. SeMet-substituted proteins were expressed as described previously (21) and purified as for the wild type protein.

Single amino acid mutations were made using the QuikChange site-directed mutagenesis kit (Stratagene). The correct sequences of the mutations were confirmed by DNA sequencing. En mutants were expressed in *E. coli* cells and purified as described for the wild type.

Crystallography—Crystals were grown at room temperature by a sitting drop vapor diffusion method, mixing 2 μl of protein solution with an equal volume of reservoir solution. The crystals of the *P*21 space group were grown over a reservoir with 20% polyethylene glycol 3350, 0.2 M ammonium sulfate, and 0.1 M MES, pH 6.0. Another crystal form (*P*43212) was grown over a reservoir containing 3 M ammonium sulfate and 0.1 M sodium citrate, pH 5.5. Both crystal forms contain one molecule in the asymmetric unit. All crystals were transferred to a

* This work was supported by a grant from the Canadian Institute of Health Research (to M. I.). The costs of publication of this article were defrayed in part by the payment of page charges. This article must therefore be hereby marked "*advertisement*" in accordance with 18 U.S.C. Section 1734 solely to indicate this fact.

The atomic coordinates and structure factors (code 1PA7 and 1UEG) have been deposited in the Protein Data Bank, Research Collaboratory for Structural Bioinformatics, Rutgers University, New Brunswick, NJ (http://www.rcsb.org/).

‡ To whom correspondence should be addressed. Tel.: 416-946-4501 (ext. 5005); Fax: 416-946-6529; E-mail: ihayashi@uhnres.utoronto.ca.

[1] The abbreviations used are: MT, microtubule; MAP, microtubule-associated protein; APC, adenomatous polyposis coli; CH domain, calponin homology domain; CAP-Gly, glycine-rich cytoskeleton-associated protein; En, EB1 MT-binding domain; MES, 4-morpholineethanesulfonic acid; PIPES, piperazine-*N*,*N'*-bis(2-ethanesulfonic acid); r.m.s.d., root-mean-square deviation.

TABLE I
Crystallographic statistics

Space group	P21				P43212
Unit cell dimensions	a = 31.9 Å, b = 48.5 Å, c = 45.0 Å, β = 103.4°				a = 48.6 Å, c = 90.3 Å
Data set	Native	Peak	Edge	Remote	
X-ray source	X8c	X8c	X8c	X8c	X12c
Wavelength (Å)	0.9800	0.9792	0.9794	0.9184	0.9790
Data range (Å)	20.0–1.45	20.0–1.8	20.0–1.8	20.0–1.8	50–2.4
Unique reflections	23798	11936	12052	15183	4615
Completeness (%)[a]	99.0 (97.8)	99.8 (99.3)	99.6 (97.9)	99.5 (96.8)	98.1 (98.2)
$I/\sigma(I)$[a]	21.1 (6.99)	26.1 (13.4)	27.3 (16.5)	26.5 (12.7)	26.4 (0.7)
R_{merge}[a,b]	0.042 (0.192)	0.041 (0.150)	0.033 (0.088)	0.035 (0.126)	0.109 (0.282)
Overall figure of merit	SOLVE 0.85 DM 0.94				
Refinement					
Resolution range (Å)	20.0–1.45				10.0–2.4
No. of reflections in working set	21093				4481
$R_{cryst}(R_{free})$[c]	0.173 (0.189)				0.223 (0.279)
r.m.s.d. bond length (Å)	0.022				0.016
r.m.s.d. bond angles (°)	1.25				1.80
No. of protein atoms	1058				977
No. of solvent atoms	136				39
No. of other atoms	10				5
Protein Data Bank accession code	1PA7				1UEG

[a] Numbers in parentheses refer to statistics for the highest shell of data.
[b] $R_{merge} = \Sigma |I_{obs} - \langle I \rangle| / \Sigma I_{obs}$, where I_{obs} is the intensity measurement and $\langle I \rangle$ is the mean intensity for multiply recorded reflections (22).
[c] R_{cryst} and $R_{free} = \Sigma \| F_{obs}| - |F_{calc}\| / |F_{obs}|$ for reflections in the working and test sets, respectively. The R_{free} value was calculated using a randomly selected 5% of the data set that was omitted through all stages of refinement.

cryosolvent containing 20% glycerol in their mother liquors and frozen in a nitrogen stream at 100 K.

All diffraction data were collected at the National Synchrotron Light Source (Brookhaven National Laboratory) on X8C and X12C beamlines using Quantum-4 CCD detectors (ADSC). Data sets were processed with DENZO and SCALEPACK (22). SOLVE was used to find selenium sites in the *P*21 crystal form and to generate the initial phases at 1.8 Å resolution. The initial phases were extended to 1.45 Å and improved by DM (23). A molecular mask was built using a solvent content of 55% in the unit cell. Initial model was built automatically with the ARP-wARP program (23). The tracing was completed using XTALVIEW (24). The model was refined by maximum-likelihood method using REFMAC5 (23). The structure of another crystal form was solved by molecular replacement with the program CNS (25) using the *P*21 crystal structure as a search model.

Microtubule Pelleting Assay—Purified tubulin (Cytoskeleton Inc.) was polymerized in PEM-G (20 mM PIPES, pH 6.8, 0.25 mM $MgCl_2$, 0.25 mM EGTA, 0.1 M NaCl, 1 mM GTP) with 10 μM taxol (Sigma) at a concentration of 50 μM for 30 min at 30 °C. Tubulin was diluted to 10 μM with PEM-G, 10 μM taxol and incubated for another 10 min. 100 μl of tubulin solution was mixed with 10 μg of En or its mutants and incubated for 30 min at room temperature. En bound to polymerized tubulin was precipitated by centrifugation through a 50% sucrose cushion for 30 min at room temperature at 90,000 rpm in an MLA-130 rotor (Beckman). After centrifugation, pellets were resuspended in SDS-PAGE loading buffer and analyzed by SDS-PAGE. Polyacrylamide gels were stained with Coomassie Brilliant Blue.

RESULTS AND DISCUSSION

Structure of En—Attempts to crystallize the human full-length EB1 protein (268 amino acids) were unsuccessful. Trypsin cleavage generated a proteolytically resistant domain, amino-terminal residues 1–130, that includes the MT-binding domain as previously reported (19, 20). This fragment formed crystals under two sets of conditions, both of which diffracted X-rays to high resolution. The initial crystals diffracted to 1.45 Å resolution, and the structure was determined by multiple wavelength anomalous diffraction (Table I) from a selenomethionine derivative. Interpretable electron density was observed for all residues. The structure of a second crystal form was determined to 2.4 Å by molecular replacement using the first structure as a search model. We could not observe ordered electron density for two loop regions located in the amino and carboxyl termini (residues 8–13 and 123–126).

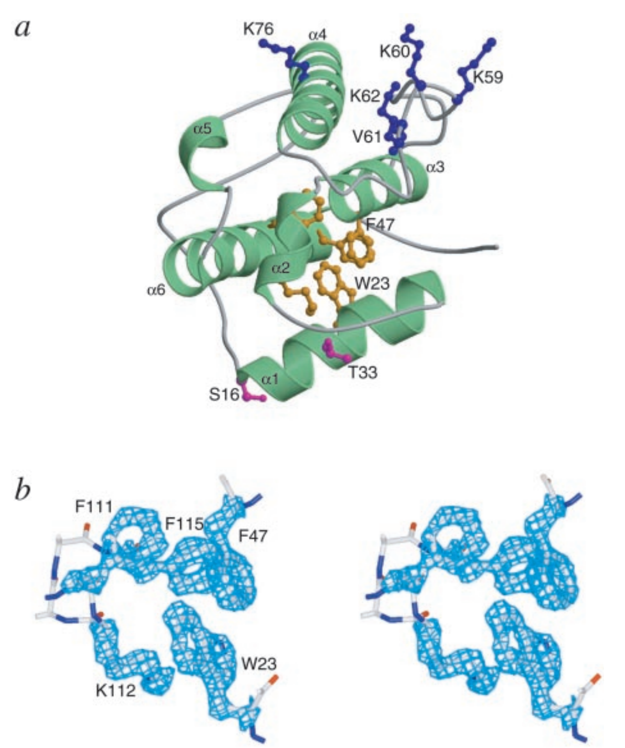

FIG. 1. **Structure of En.** *a*, schematic view of En. The basic cluster residues are shown in *ball-and-stick* form in *blue*. Hydrophobic interaction in the core region is shown in *yellow*. Ser-16 and Thr-33 are shown in *magenta*. *b*, stereo view of the experimental electron density map at the hydrophobic core superimposed on the final model. The orientation is the same as shown in *panel a*. The map is countered at 1.0 σ. This figure and Figs. 4 and 5*c* were created using MOLSCRIPT and RASTER3D (34, 35).

The En structure (Fig. 1*a*), which is globular with dimensions of 25 × 30 × 30 Å, comprises six α-helices. The archi-

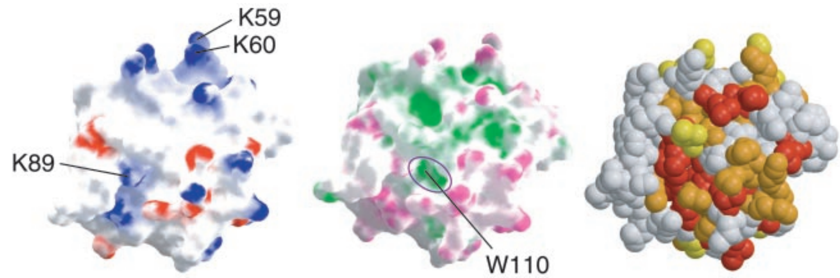

FIG. 2. **Surface properties of En.** The structure was rotated 90° clockwise about a vertical axis compared with the orientation shown in Fig. 1*a*. *Left*, electrostatic potential of En countered from −15 (*red*) to +15 (*blue*) kilotesla. *Center*, surface hydrophobicity of En. The hydrophobic area is shown in *green* and the hydrophilic in *magenta*. *Right*, sequence conservation across species: invariant (*red*), highly conserved (*orange*), conserved (*yellow*). The hydrophobic cleft is indicated by a *circle*. Surface representations were created with GRASP (36).

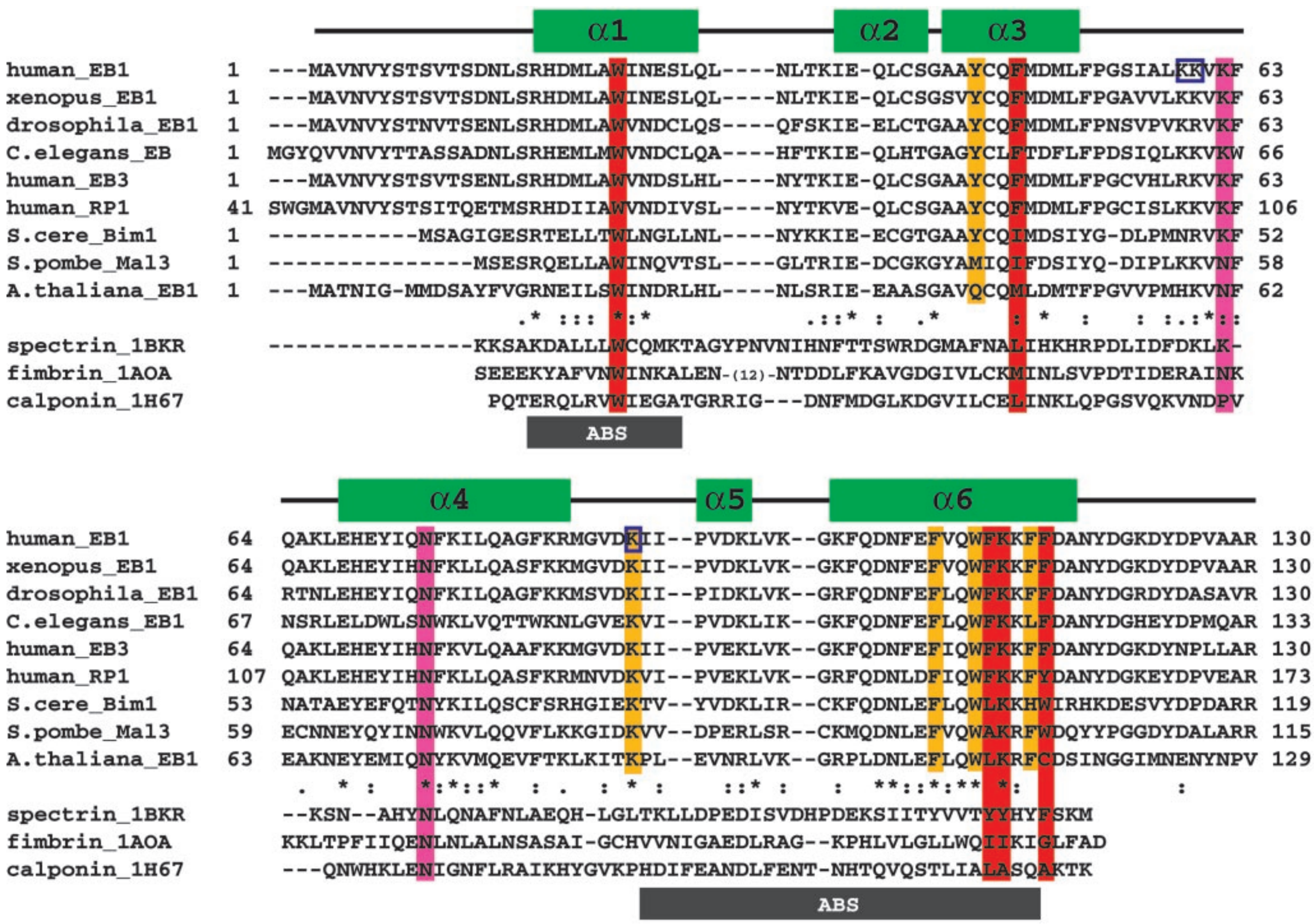

FIG. 3. **Sequence alignment of En.** En from seven different species and EB1 homologs EB3 and RP1 are aligned. Structure-based alignment with other actin-binding CH domains is shown with Protein Data Bank accession codes. Secondary structural elements are labeled above the sequences. The *gray bars* indicate actin-binding sites (*ABS*) (see text). Residues mutated in this study (Lys-59, Lys-60, and Lys-89) are *boxed* in *blue*. The residues related to Arg-89 (Tyr-44, Phe-107, Trp-110, and Phe-114) are *highlighted* in *yellow*, those related to Trp-23 (Phe-47, Phe-111, Lys-112, and Phe-115) in *red*, and to Asn-74 (Lys-62) in *magenta*.

tecture of the domain is dominated by four major α-helices (α1, α3, α4, and α6). The first helix (α1) forms an angle of ~75° with the central helices α3 and α4. Three helices, α3, α4, and α6, form a parallel three-helix bundle, giving rise to a hydrophobic core. α4 and α6 are partially exposed to the solvent, creating a conserved hydrophobic cleft that provides a potential protein interaction surface (Fig. 2). Another potential MT-binding surface consists of a basic cluster (^{59}KKVK^{62}) located in the loop between α3 and α4 together with conserved Lys-76 in α4, because many MAPs possess a basic patch and are proposed to bind to the acidic tail of tubulin (26). The backbone atoms of Lys-62 form hydrogen bonds with the side chain of invariant Asn-74 in α4 (Fig. 3), representing a rigid basic loop structure.

Structural Comparisons—Using the DALI data base (27), we found that the En structure has a calponin homology (CH) domain fold as seen in many actin-binding proteins (Fig. 4). The most closely related proteins are spectrin (Protein Data Bank code 1BKR; *Z*-score = 10.6; root-mean-square deviation (r.m.s.d.) = 2.3 Å over 97 Cα atoms; Ref. 28), fimbrin (1AOA; *Z*-score = 10.5; r.m.s.d. = 2.8 Å for 106 Cα; Ref. 29), and calponin (1H67; *Z*-score = 9.6; r.m.s.d. = 2.9 for 103 Cα; Ref. 30). The core structure is conserved among all the CH domains, except En has extra residues at its amino and carboxyl termini.

A tandem pair of CH domains, each consisting of about 100 amino acids, has been suggested to confer actin binding on a variety of cytoskeletal and signaling events (31). Although a BLAST search against EB1 failed to find sequence similarity

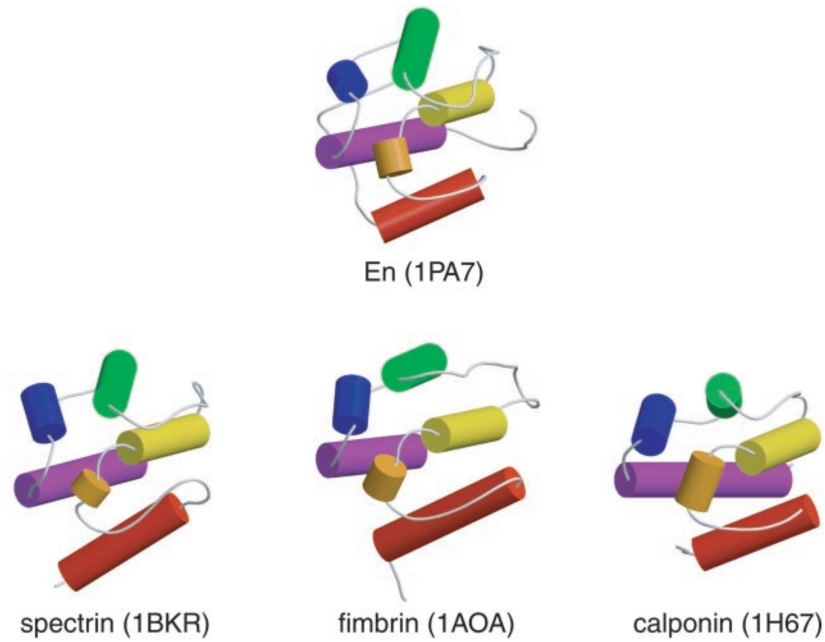

FIG. 4. **Structural comparisons of En.** En structure is compared with domains of spectrin, fimbrin, and calponin. Protein Data Bank codes are shown in parentheses. Orientations are the same as in Fig. 1*a*. Helices are colored from the amino terminus: *red*, *orange*, *yellow*, *green*, *blue*, and *purple*.

with other CH domains, some of the aromatic residues in the En core region are conserved throughout the CH domain family (Fig. 3), suggesting that they are essential for maintaining the tertiary structure. In particular, Trp-23 in EB1 is identical within the CH domain family (30). The aromatic ring of Trp-23 forms nonpolar interactions with the aliphatic side chain of Lys-112 and the aromatic ring of Phe-115 (Fig. 1*b*). Lys-112 and Phe-115 are mostly conserved as the hydrophobic residues in the EB1 family.

Potential Phosphorylation Sites—In our crystal structure, we found that Ser-16 and Thr-33 are exposed to solvent (Fig. 1*a*). Ser-16 locates to the entrance of α1 and is found in all species studied except for *Arabidopsis thaliana*. Ser-16 resides within the recognition sequence of protein kinase CKI/II, such that Ser-16 could be one of the determinants to regulate MT movement by phosphorylation. Thr-33, which lies in the loop region between α1 and α2, is conserved as Thr or Ser in many species. However, this residue does not belong to any known kinase recognition sequence predicted from NetPhos2.0 (www.cbs.dtu.dk/services/NetPhos/). The remaining Ser and Thr residues are mostly buried in the molecule and vary among the species. Thus far phosphorylation sites of EB1 have not been reported, and the kinase regulation of EB1 still remains in question.

Microtubule Binding—MT-binding motifs have a net positive charge that is thought to be important for binding to the acidic carboxyl-terminal region of tubulin. This acidic region is located on the outer surface of microtubules, providing an accessible site for MAPs (26). On the other hand, the actin-binding sites in many CH domains are predominantly hydrophobic in nature (29, 32), which correspond to α1 of the first CH domain of the tandem repeat and α5 and α6 of the second repeat (Fig. 3). From our crystal structure, we predict two potential MT-binding sites: one involving the loop region with the basic cluster between α3 and α4 and another within the conserved hydrophobic cleft encompassed by α5 and α6.

To investigate whether the interaction between EB1 and MTs is electrostatic, we tested MT-binding ability with various salt concentrations (Fig. 5*a*). En co-sedimented with MTs at physiological ionic strength (NaCl = 150 mM). On increasing the salt concentration above 200 mM, En could not bind MTs. This observation suggests that the binding affinity is, at least in part, electrostatic.

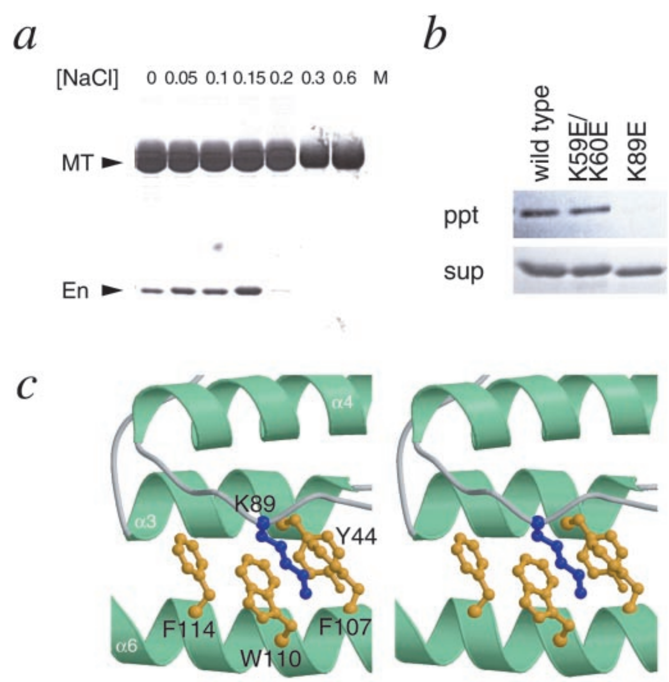

FIG. 5. **Interaction of En with MTs.** *a*, co-sedimentation of En with MTs in various salt concentrations. Over the range of physiological salt concentration (≥0.2 M NaCl), En cannot co-sediment with MTs. *b*, mutational analysis of the interaction between En and MTs. En bound to MTs is shown in the *upper section*, whereas the *lower section* shows the supernatant of the co-sedimentation assay. *c*, stereo view of the environment of Lys-89. Lys-89 is colored in *blue*, and the surrounding hydrophobic residues are in *yellow*.

To define the MT-binding site on En, we made double and single mutants (K59E/K60E and K89E) to give a strong electrostatic effect on En. Lys-59 and Lys-60 are located in the basic cluster, whereas Lys-89 is close to the hydrophobic cleft described above. Mutants were correctly folded as judged by circular dichroism spectroscopy. Wild type and K59E/K60E co-sedimented with MTs, whereas K89E abolished binding (Fig. 5*b*). Our crystal structure shows that the surrounding environment of highly conserved Lys-89 is identical and hydrophobic in EB1 (Fig. 5*c*); its aliphatic side chain is located in the middle of the aromatic stack of Phe-107, Trp-110, and Phe-114. Phe-107 forms a further nonpolar interaction with Phe-44. In addition, the mutation of invariant Trp-110 causes a destabilization of En structure, resulting in the loss of expression in *E. coli* cells. Taken together, we propose that En utilizes the hydrophobic network for MT binding as well as for the maintenance of the CH domain structure.

A yeast genetic study of the EB1 homolog BIM1 suggested that the locus of the interaction is near the carboxyl terminus of α-tubulin (13). Our data show that En binding is electrostatic but also suggest that the solvent-exposed hydrophobic patch may be the main binding site for MTs. The sequence of the α-tubulin tail (^{399}EEEGEEY^{405}) has a conserved aromatic residue at the carboxyl terminus, which may serve as a potential anchor for the hydrophobic interaction.

A recent crystal structure of another MT plus-end-binding motif, the CAP-Gly domain, revealed no structural similarity with En (33). In the CAP-Gly domain structure, an invariable sequence is located in a groove surrounded by β-sheets, which is proposed to mediate MT binding. It should be noted that there is a conserved hydrophobic cluster within the groove. Further mutagenesis or structural analysis is required to determine a common mechanism of plus-end binding.

The CH domain architecture is emerging as a filamentous protein interaction module in a number of cytoskeletal proteins. In previous reports, the functional CH domain for actin binding is suggested to be a tandem pair, whereas the actin-binding ability of the single CH domain is still ambiguous (30, 32). En is the first example of a single CH domain that can bind to the cytoskeletal filament. We propose that, similar to actin-binding CH domains, En employs predominantly hydrophobic interactions to bind to MTs.

Acknowledgments—We thank Drs. Jose M. Pereda and Yuko Mimori-Kiyosue for critical reading of the manuscript and the staff at the Brookhaven National Laboratory for synchrotron access.

REFERENCES

1. Desai, A., and Mitchison, T. J. (1997) *Annu. Rev. Cell Dev. Biol.* **13,** 83–117
2. Mitchison, T., and Kirschner, M. (1984) *Nature* **312,** 237–242
3. Desai, A., Verma, S., Mitchison, T. J., and Walczak, C. E. (1999) *Cell* **96,** 69–78
4. Schuyler, S., and Pellman, D. (2001) *Cell* **105,** 421–424
5. Perez, F., Diamantopoulos, G. S., Stalder, R., and Kreis, T. E. (1999) *Cell* **96,** 517–527
6. Vaughan, K. T., Tynan, S. H., Faulkner, N. E., Echeverri, C. J., and Vallee, R. B. (1999) *J. Cell Sci.* **112,** 1437–1447
7. Berrueta, L., Kraeft, S. K., Tirnauer, J. S., Schuyler, S. C., Chen, L. B., Hill, D. E., Pellman, D., and Bierer, B. E. (1998) *Proc. Natl. Acad. Sci. U. S. A.* **95,** 10596–10601
8. Schroer, T. A. (2001) *Curr. Opin. Cell Biol.* **13,** 92–96
9. Ligon, L. A., Shelly, S. S., Tokito, M., and Holzbaur, E. L. (2003) *Mol. Biol. Cell* **14,** 1405–1417
10. Su, L. K., Burrell, M., Hill, D. E., Gyuris, J., Brent, R., Wiltshire, R., Trent, J., Vogelstein, B., and Kinzler, K. W. (1995) *Cancer Res.* **55,** 2972–2977
11. Kinzler, K. W., and Vogelstein, B. (1996) *Cell* **87,** 159–170
12. Beinhauer, J. D., Hagan, I. M., Hegemann, J. H., and Fleig, U. (1997) *J. Cell Biol.* **139,** 717–728
13. Schwartz, K., Richards, K., Botstein, D. (1997) *Mol. Biol. Cell* **8,** 2677–2691
14. Morrison, E. E., Wardleworth, B. N., Askham, J. M., Markham, A. F., and Meredith, D. M. (1998) *Oncogene* **17,** 3471–3477
15. Juwana, J. P., Henderikx, P., Mischo, A., Wadle, A., Fadle, N., Gerlach, K., Arends, J. W., Hoogenboom, H., Pfreundschuh, M., and Renner, C. (1999) *Int. J. Cancer* **81,** 275–284
16. Askham, J. M., Moncur, P., Markham, A. F., and Morrison, E. E. (2000) *Oncogene* **19,** 1950–1958
17. Mimori-Kiyosue, Y., Shiina, N., and Tsukita, S. (2000) *Curr. Biol.* **10,** 865–868
18. Nakamura, M., Zhou, X. Z., and Lu, K. P. (2001) *Curr. Biol.* **11,** 1062–1067
19. Barth, A. I., Siemers, K. A., and Nelson, W. J. J. (2002) *Cell Sci.* **115,** 1583–1590
20. Askham, J. M., Vaughan, K. T., Goodson, H. V., and Morrison, E. E. (2002) *Mol. Biol. Cell* **13,** 3627–3645
21. Harrison, C. J., Bohm, A. A., and Nelson, H. C. M. (1994) *Science* **263,** 224–227
22. Otwinowski, Z., and Minor, W. (1997) *Methods Enzymol.* **227,** 366–396
23. Collaborative Computational Project, Number 4 (1994) *Acta Crystallogr. Sect. D Biol. Crystallogr.* **50,** 760–763
24. McRee, D. E. (1999) *J. Struct. Biol.* **125,** 156–165
25. Brünger, A. T., Adams, P. D., Clore, G. M., Gros, P., Grosse-Kunstleve, R. W., Jiang, J.-S., Kuszewski, J., Nilges, M., Pannu, N. S., Read, R. J., Rice, L. M., Simonson, T., and Warren, G. L. (1998) *Acta Crystallogr. Sect. D Biol. Crystallogr.* **54,** 905–921
26. Nogales, E., Whittaker, M., Milligan, R. A., and Downing, K. H. *Cell* **96,** 79–88
27. Holm, L., and Sander, C. (1997) *Nucleic Acids Res.* **25,** 231–234
28. Banuelos, S., Saraste, M., and Carugo, K. D. (1996) *Structure* **6,** 1419–1431
29. Goldsmith, S. C., Pokala, N., Shen, W., Fedorov, A. A., Matsudaira, P., and Almo, S. C. (1997) *Nat. Struct. Biol.* **4,** 708–712
30. Bramham, J., Hodgkinson, J. L., Smith, B. O., Uhrin, D., Barlow, P. N., and Winder, S. J. (2002) *Structure* **10,** 249–258
31. Castresana, J., and Saraste, M. (1995) *FEBS Lett.* **374,** 149–151
32. Gimona, M., Djinovic-Carugo, K., Kranewitter, W. J., and Winder, S. J. (2002) *FEBS Lett.* **513,** 98–106
33. Li, S., Finley, J., Liu, Z. J., Qiu, S. H., Chen, H., Luan, C. H., Carson, M., Tsao, J., Johnson, D., Lin, G., Zhao, J., Thomas, W., Nagy, L. A., Sha, B., DeLucas, L. J., Wang, B. C., and Luo, M. (2002) *J. Biol. Chem.* **277,** 48596–48601
34. Kraulis, P. J. (1991) *J. Appl. Crystallogr.* **24,** 946–950
35. Merrit, E. A., and Murphy, M. E. P. (1994) *Acta Crystallogr. Sect. D Biol. Crystallogr.* **50,** 869–873
36. Nicholls, A., Sharp, K. A., and Honig, B. (1991) *Proteins* **11,** 281–296